**Trabajos de Geología**, Universidad de Oviedo, 29 : 297-302 (2009)

Oviedo (Spain)
1-3 July 2008
International Meeting of Young Researchers in Structural Geology and Tectonics
ORSGET

# Numerical modeling of interplay between growth folds and fluvial-alluvial erosion-sedimentation processes

V. H. García[1, 2, 3*] and E. O. Cristallini[1, 2]

[1] *Laboratorio de Modelado Geológico, Departamento de Ciencias Geológicas, Facultad de Ciencias Exactas y Naturales, Universidad de Buenos Aires. Pabellón II, Ciudad Universitaria, C1428EGA, Ciudad Autónoma de Buenos Aires, Argentina.*

[2] *Consejo Nacional de Investigaciones Científicas y Técnicas, Avda. Rivadavia 1917, C1033AAJ, Ciudad Autónoma de Buenos Aires, Argentina.*

[3] *Now at: Instituto de Bio y Geociencias (CONICET-UNSa), Av. Bolivia 5150 (4400) Salta, Argentina.*

**e-mail: victorg@conicet.gov.ar*

---

**Abstract:** The main aim of the present study is to model the interplay between neotectonic growth folds and fluvial-alluvial processes in piedmont areas using an original numerical modeling platform (ERSEDE). ERSEDE allows the quantifying of topographic changes in the model along its evolution. The model outputs can be used to carry out detailed analysis on growth strata geometries and geomorphic evolution. The application of models to analyze this kind of interplays is an important tool to understand the evolution of mountain fronts and it can be helpful to calibrate deformation and denudation rates obtained from neotectonic features.

**Keywords:** numerical modelling, tectonic geomorphology, growth folds, fluvial-alluvial processes, mountain front.

---

The numerical modeling of fluvial erosion-transport-sedimentation processes has been object of intense research in the last years (see Whipple, 2004, for a synthesis). The stream power models have demonstrated to be the most efficient for simulating fluvial processes in mountainous environments (Howard and Kerby, 1983; Whipple and Tucker, 1999, Tucker and Bras, 2000; Whipple and Tucker, 2002). Bedrock-rivers are the dominant ones in these kinds of regions (Howard, 1980; Howard *et al.*, 1994) and are characterized by bedrock exposures along almost all the river path, with some sectors covered by transient sediments.

Once the rivers reach the piedmont its erosion and transport capacity is rapidly reduced by the slope decrease, developing alluvial fans in the mountain front mainly controlled by discharge events repeated through time (Harvey *et al.*, 2005). Neotectonic features (fault scarps, growth folds, etc.) are frequently found in the piedmont of the active mountain chains as direct evidence of deformation propagation and recent tectonic activity. The geomorphologic characteristics of those features are used to establish the level of activity of the system (Keller and Pinter, 1996; Burbank and Anderson, 2001). The growth strata derived from the interaction between the growing structures and alluvial processes represent an important tool to analyze the temporal evolution of the structures and the deformation rates (Burbank and Vergés, 1994; Ford *et al.*, 1997).

In this contribution, a hypothetical fold growing in the piedmont of the Andean orogenic front was analyzed for a 10,000 years forward evolution. The results show that the presented numerical modeling platform, named ERSEDE (García, 2010), is a useful tool to analyze the interaction between neotectonics and surface processes.

## Study area

The study area is located near to the orogenic front of the Andes, at the eastern flank of the Precordillera between 68º51' and 69º09' LW and 32º30' and 32º41' LS in the Mendoza province of Argentina (Fig. 1). The hypothetical growth anticline was disposed with N-S trend in the Pampa Rodeo Grande, which is the present *bajada* of the mountain range. The Canota and del Toro creeks are the main rivers that drain the mountainous area, cross the Pampa Rodeo Grande and reach the Las Higueras river.

The Silurian-Devonian greenish sandstones and mudstones of the Villavicencio Group (Cuerda *et al.*, 1988) are the dominant lithology of this sector of the Precordillera. These rocks are deformed and can develop low-grade metamorphism. Overlying this unit there are volcanic and pyroclastic rocks of the Choiyoi Group (Permo-Triassic, Rolleri and Criado Roque, 1968), and sedimentary continental deposits of the Uspallata Group (Middle to Upper Triassic, Kokogian and Mansilla, 1989). In the western flank of the Higueras range, toward the NE corner of the sector, outcrops of the Uspallata Group are recognized. The climate of the region is arid with annual precipitations lower than 350-400 mm. The rivers are ephemerals, being active only during the rainy season. These rivers can transport great amounts of materials during floods.

The intense seismic activity (INPRES, 1995) and the presence of neotectonic structures as the La Cal fault scarp (Mingorance, 2006) and the Borbollón-Capdeville growth folds (Costa *et al.*, 2000) are markers of Quaternary tectonic activity in the area.

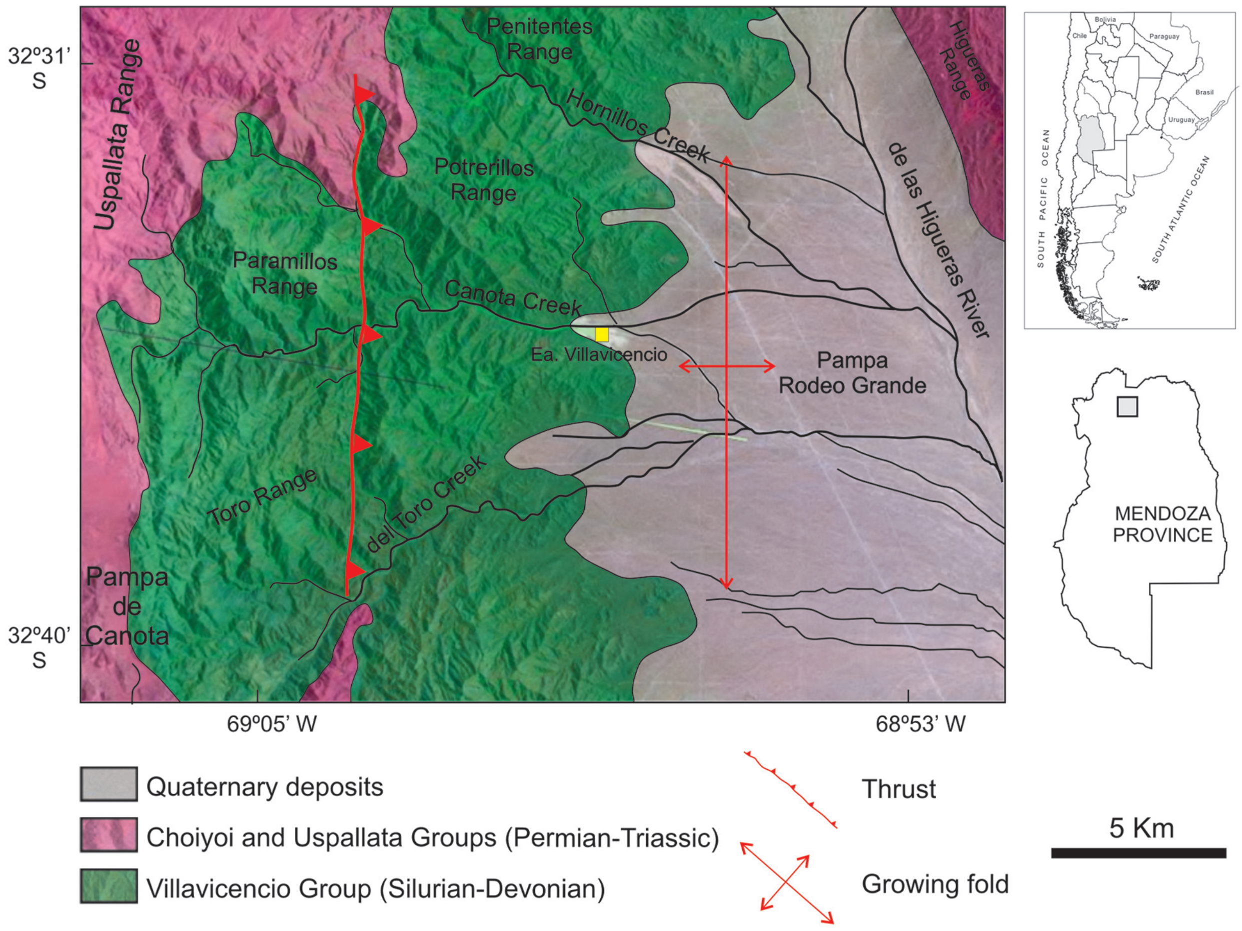

**Figure 1.** Landsat image of the study area with basic geology superimposed. The position of the modeled growth fold is indicated using an anticline reference.

## Methodology

### *Modeling of fluvial-alluvial processes*

The numerical models that simulate landscape evolution are generally designed using empirical relationships and simplifications derived from engineering transport laws (Willgoose *et al.*, 1991; Howard *et al.*, 1994; Tucker and Slingerland, 1996; Whipple and Tucker, 1999). The erosion capacity ($E$) of a river at one point of its path can be determined from the following algorithm:

$$E = (S^m\, Q^n\, K_e) - (Q_s + T) \qquad (1),$$

where $S$ is the local slope, $Q$ is the water discharge, $K_e$ is the rock erodibility, $Q_s$ is the sediment charge in transport, and $T$ is a threshold for fluvial erosion. The exponents $m$ and $n$ have been obtained from previous works (Whipple and Tucker, 1999, Clevis *et al.*, 2003), having values of 0.66 and 0.33 respectively.

The water discharge ($Q$) is obtained from the next formulae:

$$Q = A\, P^{0.65} \qquad (2),$$

where $A$ is the upstream drainage area, and $P$ is the precipitation. A straight corollary from the equation (1) is that erosion will take place only when the result is positive.

The erodibilities ($K_e$) for different lithologies have been calibrated using denudation rates at short temporal scales in the Bolivian Andes (Aalto *et al.*, 2006). The obtained results are summarized in the table 1.

When the transport capacity is exceeded by the sediment charge, the river must leave some material. The quantity of released material is a function of the available accommodation space. The material added to the old topography can not exceed the actualized topography of the immediately previous point in the river path. The limit will be controlled by the slope of the point of interest with respect of the next point in the river path. In addition, sedimentation can not generate depressions or increase slopes. This process continues until the river recovers its transport-erosion capacity, or until the end of the river path.

### *Modeling of growth folds*

The program ERSEDE includes a module to simulate the growth of an anticline structure on a previous real (DEM's) or artificial topography. The growth of the fold is controlled by the fault-parallel flow kinematic model (Sanderson, 1982). The requested input data includes the fault geometry (dip, depth of detachment, vergence), the shortening rate and the recurrence interval.

### *Model parameters*

A model of 100 steps was executed with the parameters detailed in table 2. An erodibility of $3000\times10^{-7}$ $m^2\ a^{-1}$ was assigned for all the pre deformation topography, without taking into account the presence of Quaternary cover. This value is the average erodibility determined for metasedimentary and weak sedimentary rocks in the work of Aalto *et al.* (2006) (Table 1).

The geometry of the fault is in agreement with other examples of folds in the orogenic front (García *et al.*, 2005). In order to obtain a double plunging anticline the displacement over the fault plane has been distributed from 2 mm $a^{-1}$ in the center of the fault up to 0 mm $a^{-1}$ at both ends of the fault. The shortening rate is coherent with rates obtained for similar structures in the region (Vergés *et al.*, 2007).

## Results, discussion and limitations

The progressive growth of the anticline can be observed in the topographic evolution of the region. Two N-S scarps are cutting the piedmont. The western scarp represents the backlimb of the anticline and the eastern scarp the forelimb. The area between both scarps is the crest of the fold (Fig. 2a). Straight scarps related to fold axial surfaces are not commonly developed in real examples, reflecting the instantaneous limb rotations

| Basin | Area ($km^2$) | Precipitation (mm $a^{-1}$) | Lithology | PLI Index | Denudation rate (mm $a^{-1}$) | Erodibility best fit ($10^{-7}$ $m^2$ $a^{-1}$) |
|---|---|---|---|---|---|---|
| VIN | 50 | 510 | Igneous-metamorphic basement | 4.0 | 0.02 | **209** |
| ELV | 64 | 250 | Metasedimentary | 4.8 | 0.18 | **2200** |
| ACH | 38 | 170 | Weak sedimentary | 34.0 | 2.00 | **3910** |

**Table 1.** Erodibility values assigned to the lihology-types studied by Aalto *et al.* (2006). The PLI index represents the rupture resistance of fresh rocks using the Schmidt N-type hammer.

| **Physical parameters** | | | | | |
|---|---|---|---|---|---|
| Topography | Precipitation (mm a$^{-1}$) | Bedrock erodibility ($10^{-7}$ m$^2$ a$^{-1}$) | Sediments erodibility ($10^{-7}$ m$^2$ a$^{-1}$) | Dimensions (pixels) | Step (years) |
| SRTM DEM 90m | 300 | 3000 | 1 000 000 | 294×223 | 100 |
| **Fault parameters** | | | | | |
| Detachment depth (km) | Dip (degrees) | Vergence | Recurrence interval (years) | Shortening rate (mm a$^{-1}$) | Ramp dimensions (km) |
| -10 | 30 | East | 1000 | 5 | 13.5×3.375 |

**Table 2.** Model parameters.

intrinsic of the applied deformation model. The pre-deformation surface is partially preserved in the crest zone, being progressively degraded (Fig. 2d). This kind of surfaces (or pediments) is a common feature in the Andean piedmont at these latitudes (e.g. García *et al.*, 2005). The path of the rivers in the piedmont changes along the model evolution, but without development of abrupt bends (Fig. 2b). The path changes could be controlled by alluvial autocyclic avulsion processes, being the uplift rate too low to establish barriers to the rivers. Erosion concentrates in the mountainous areas with high slopes and in the frontal scarp of the fold. The sedimentation in the mountain bedrock channels is transient, without great accumulations (Fig. 2c). Sedimentation dominates in the piedmont, showing a distributary character along the model evolution (Fig. 2c). This behavior can be correlated with the processes responsible for the construction of alluvial fans (Harvey *et al.*, 2005).

The growth strata evolution across the fold (Fig. 3) shows active sedimentation above both flanks covering the fold crest. This geometry of rotational onlap (Riba, 1976) indicates that the sedimentation rate is surpassing the uplift rate hiding the morphostructural response of the landscape. The obtained growth strata geometry is different and more complex than those modeled for longer time spans using simple "table"

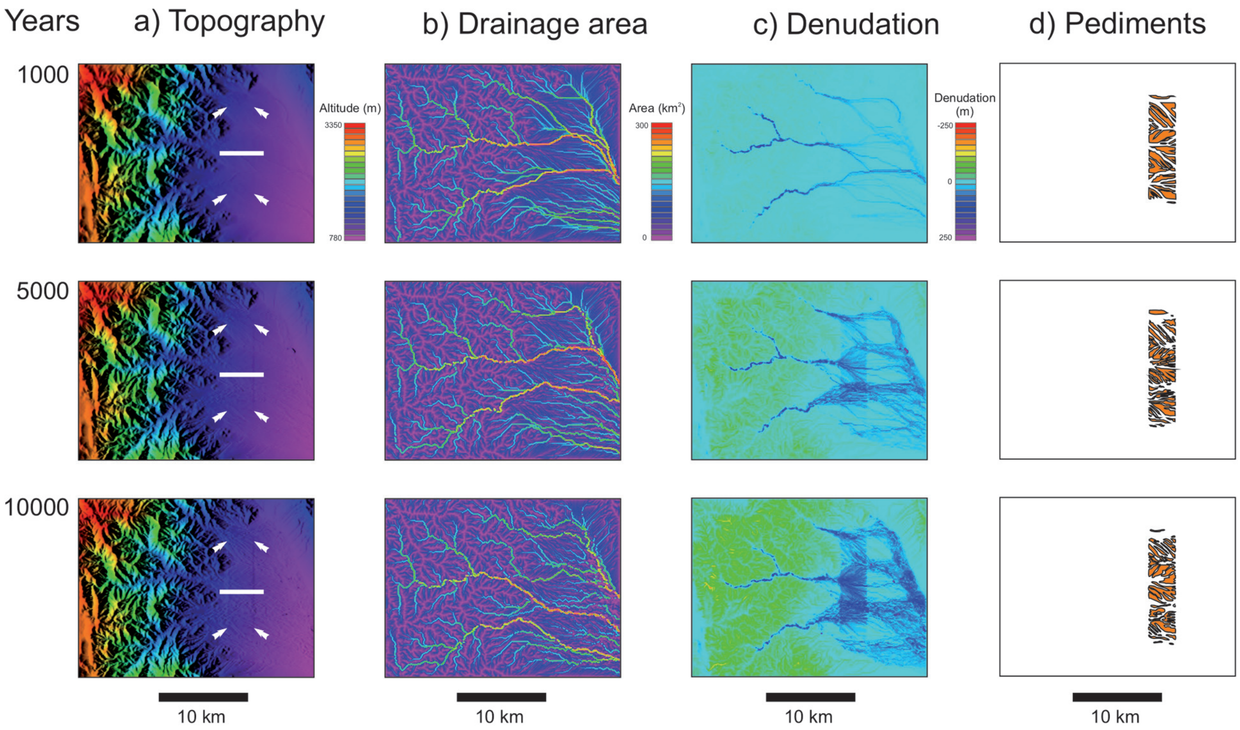

**Figure 2.** Temporal evolution of the model showing: (a) fold growth (white arrows mark the position of the scarps), (b) variability of the drainage network, (c) denudation patterns, and (d) progressive degradation of pre-deformation surfaces (pediments). The location of the growth strata profiles is marked with white bars in the topographic scenes.

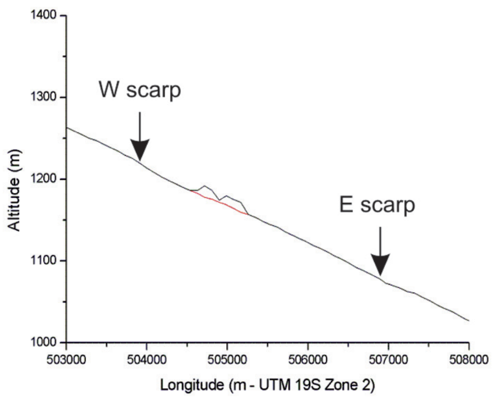

1000 years

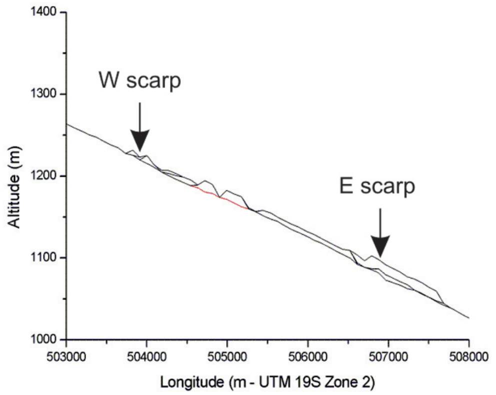

5000 years

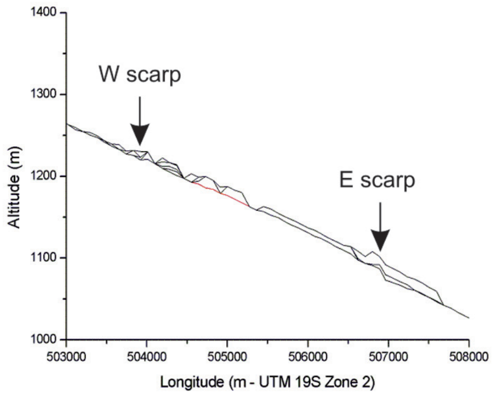

10000 years

**Figure 3.** Growth strata geometry in the central sector of the fold with a vertical exaggeration of 10×. Observe the rotational onlap in the scarp zones. The position of the profiles is indicated in the figure 2.

geometry for sedimentation and can be useful to analyze growth patterns in Quaternary deposits.

The limitations of the model are related with the “rectangular” geometry of the growing fold and the spatial resolution of the grid. The geometry of the fold is controlled by the algorithm of fault-parallel flow applied and can be improved using more realistic algorithms (i.e. trishear). The spatial resolution of the grid is limited by the computational time necessary to run the simulations. For a 300×300 pixels grid the program spent 2 or 3 days to obtain satisfactory results.

Another more general limitation is the algorithm used to model river erosion and sedimentation based in geometrical and empirical parameters. More studies are needed to obtain process-based models.

## Conclusions

The interaction between a growth anticline and the fluvial-alluvial processes was successfully modeled. Geomorphic markers of neotectonic activity (pediments and scarps) were obtained along the model evolution. In the model, alluvial sedimentation in the piedmont was controlled by avulsion and abandon of individual channels. ERSEDE proved to be able to simulate the development of alluvial fans. The shortening rate and the recurrence interval applied are not enough to modify the general design of the drainage network, at least for the time span analyzed in this paper. The interaction between deformation and alluvial processes in the scarp zones produced rotational onlap growth strata geometries.

The obtained results indicate that the program ERSEDE is a valid tool to simulate the interplay between neotectonic and fluvial-alluvial erosion-sedimentation processes.

## References

Aalto, R., Dunne T. and Guyot, J. L. (2006): Geomorphic controls on Andean denudation rates. *J. Geol.*, 114: 85-99.

Burbank, D. W. and Anderson, R. S. (2001): *Tectonic geomorphology*. Blackwell Science, Malden, 274 pp.

Burbank, D. W. and Vergés, J. (1994): Reconstruction of topography and related depositional systems during active thrusting. *J. Geophys. Res.*, 90: 20281-20297.

Clevis, Q., de Boer, P. and Wachter, M. (2003): Numerical modelling of drainage basin evolution and three-dimensional alluvial fan stratigraphy. *Sediment. Geol.*, 163: 85-110.

Costa, C., Gardini, C., Diederix, H. and Cortes, J. (2000): The Andean thrust front at Sierra de las Peñas, Mendoza, Argentina. *J. S. Am. Earth Sci.*, 13: 287-292.

CUERDA, A. J., LAVANDAIO, E., ARRONDO, O. and MOREL, E. (1988): Investigaciones estratigráficas en el Grupo Villavicencio, Canota, prov. de Mendoza. *Rev. Asoc. Geol. Argent.*, 43, 3: 356–365.

FORD, M., WILLIAMS, E. A., ARTONI, A., VERGÉS, J. and ARDÍ, S. (1997): Progressive evolution of a fault-related fold pair from growth strata geometries, Sant Llorenc de Morunys, SE Pyrenees. *J. Struct. Geol.*, 19, 3-4: 413-441.

GARCÍA, V. H. (2010): *Modelado de las interacciones entre procesos de erosión y sedimentación fluvial y el crecimiento de estructuras neotectónicas*. PhD Thesis, Universidad de Buenos Aires, Argentina, 218 pp.

GARCÍA, V. H., CRISTALLINI, E. O., CORTÉS, J. M. and RODRÍGUEZ, M. C. (2005): Structure and neotectonics of Jaboncillo and del Peral anticlines. New evidences of Pleistocene to Holocene deformation in the Andean piedmont? *6th International Symposium of Andean Geodynamics, Extended Abstracts*, 301-304.

HARVEY, A. M., MATHER, A. E. and STOKES, M. (2005): Alluvial Fans: Geomorphology, Sedimentology, Dynamics. *Geol. Soc. London Spec. Publ.*, 251.

HOWARD, A. D. (1980): Thresholds in river regimes. In: D. R. COATES and J. D. VITEK (eds): *Thresholds in Geomorphology*, 227-258. Boston.

HOWARD, A. D. and KERBY, G. (1983): Channel changes in badlands. *B. Geol. Soc. Am.*, 94: 739-752.

HOWARD, A. D., SEIDL, M. A. and DIETRICH, W. E. (1994): Modeling fluvial erosion on regional to continental scales. *J. Geophys. Res.*, 99: 13971-13986.

INPRES (1995): *Microzonificacion sísmica del gran Mendoza: Executive abstract*, Technical publication, 19.

KELLER, E. A. and PINTER, N. (1996): *Active tectonics: earthquakes, uplift and landscape*. Prentice Hall, New Jersey, 338 pp.

KOKOGIAN, D. and MANSILLA, O. (1989): Análisis estratigráfico secuencial de la Cuenca Cuyana. In: G. CHEBLI and L. SPALLETTI (eds): *Cuencas Sedimentarias Argentinas*, Universidad Nacional de Tucumán, Serie Correlación Geológica, 6: 169-210.

MINGORANCE, F. (2006): Morfometría de la escarpa de falla histórica identificada al norte del cerro La Cal, zona de falla La Cal, Mendoza. *Rev. Asoc. Geol. Argent.*, 61, 4: 620-638.

RIBA, O. (1976): Syntectonic unconformities of the Alto Cardener, Spanish Pyrenees: A genetic interpretation. *Sediment. Geol.*, 15: 213-233.

ROLLERI, E. and CRIADO ROQUE, P. (1968): La Cuenca triásica del norte de Mendoza. *Terceras Jornadas Geológicas Argentinas*, 1: 1-76.

SANDERSON, D. J. (1982). Models of strain variation in nappes and thrust sheets; a review. *Tectonophysics*, 88: 201-233.

TUCKER, G. E. and BRAS, R. L. (2000): A stochastic approach to modeling the role of rainfall variability in drainage basin evolution. *Water Resour. Res.*, 34: 1953-1964.

TUCKER, G. E. and SLINGERLAND, R. (1996): Predicting sediment flux from fold and thrust belts. *Basin Res.*, 8: 329-349.

VERGÉS, J., RAMOS, V. A., MEIGS, A., CRISTALLINI, E. O., and CORTES, J. M. (2007): Crustal wedging triggering recent deformation in the Andean thrust front between 31º S and 33º S: Sierras Pampeanas - Precordillera interaction. *J. Geophys. Res.*, 112: B03S15.

WHIPPLE, K. (2004): Bedrock rivers and the geomorphology of active orogens. *Annu. Rev. Earth Pl. Sc.*, 32: 151-185.

WHIPPLE, K. and TUCKER, G. (1999): Dynamics of the stream-power river incision model: implications for height limits of mountain ranges, landscape response, and research needs. *J. Geophys. Res.*, 104: 17661-17674.

WHIPPLE, K. and TUCKER, G. (2002): Implications of sediment-flux dependent river incision models for landscape evolution. *J. Geophys. Res.*, 107. doi: 10.1029/2000JB000044.

WILLGOOSE, G., BRAS, R. L., and RODRÍGUEZ-ITURBE, I. (1991): A coupled channel network growth and hillslope evolution model. 1. Theory. *Water Resour. Res.*, 30: 151-159.